

Global Biogeochemical Cycles

Supporting information for

Arctic permafrost thawing enhances sulfide oxidation

Preston C. Kemeny^{1,2*}, Gen K. Li^{2,3}, Madison Douglas², William Berelson⁴, Austin J. Chadwick², Nathan F. Dalleska², Michael P. Lamb², William Larsen⁵, John S. Magyar², Nick E. Rollins⁴, Joel Rowland⁶, M. Isabel Smith⁴, Mark A. Torres⁵, Samuel M. Webb⁷, Woodward W. Fischer², A. Joshua West⁴

¹ Department of the Geophysical Sciences, University of Chicago, Chicago, Illinois, USA

² Division of Geological and Planetary Sciences, California Institute of Technology, Pasadena, California, USA

³ Department of Earth Science, University of California Santa Barbara, Santa Barbara, USA

⁴ Department of Earth Sciences, University of Southern California, Los Angeles, California, USA

⁵ Department of Earth, Environmental, and Planetary Sciences, Rice University, Houston, Texas, USA

⁶ Earth and Environmental Sciences Division, Los Alamos National Laboratory, Los Alamos, New Mexico, USA

⁷ Stanford Synchrotron Radiation Lightsource, SLAC National Accelerator Laboratory, Menlo Park, California, USA

*Corresponding author: preston.kemeny@gmail.com

Contents of this file

Appendix S1 to S4

Tables S1 to S3

Figures S1 to S25

Table of Contents:

Appendices

| | |
|--|----|
| Appendix S1: Ion chromatography | 3 |
| Appendix S2: Field context and data analysis | 4 |
| Appendix S3: Additional inversion results | 13 |
| Appendix S4: Review of selected prior fluvial observations in the Yukon River Basin | 22 |

Tables

| | |
|---|----|
| Table S1: Precision of ion chromatography measurements..... | 3 |
| Table S2: Inversion-constrained end-member contributions to river dissolved load | 13 |
| Table S3: Selected prior work on seasonal and annual changes in permafrost river solutes | 27 |

Figures

| | |
|---|----|
| Fig. S1: Drone photographs of the Koyukuk River and surrounding floodplain near Huslia | 4 |
| Fig. S2: Influence of collection bottle on major ion concentrations | 6 |
| Fig. S3: Precipitation major ion ratios | 7 |
| Fig. S4: $\delta^{34}\text{S}_{\text{SO}_4}$ mixing diagrams..... | 8 |
| Fig. S5: Sedimentary sulfur and carbon isotope ratios | 9 |
| Fig. S6: SO_4^{2-} concentration and $\delta^{34}\text{S}_{\text{SO}_4}$ values along pore fluid transect | 10 |
| Fig. S7: $\delta^{18}\text{O}_{\text{H}_2\text{O}}$ and $\delta\text{D}_{\text{H}_2\text{O}}$ measurements..... | 11 |
| Fig. S8: Concentration-discharge relationships for Ca^{2+} , Mg^{2+} , Na^+ , K^+ , SO_4^{2-} , and Cl^- | 12 |
| Fig. S9: Inversion-constrained end-member chemistry..... | 14 |
| Fig. S10: Median end-member contributions, scenario 1 (without degassing)..... | 15 |
| Fig. S11: Median end-member contributions, scenario 2 (with degassing at $< 2.5x$ DIC) | 16 |
| Fig. S12: Median end-member contributions, scenario 3 (with degassing at $< 25x$ DIC) | 17 |
| Fig. S13: Median end-member contributions, scenario 4 (degassing fractionation -20‰ to 0‰) .. | 18 |
| Fig. S14: Median end-member contributions, scenario 5 (degassing fractionation -10.1‰ to 0‰) | 19 |
| Fig. S15: Sensitivity of inversion results to magnitude of degassing..... | 20 |
| Fig. S16: Sensitivity of inversion results to degassing fractionation factor | 21 |
| Fig. S17: Prior observations from the CPCRW (Maclean et al., 1999; Petrone et al., 2006)..... | 28 |
| Fig. S18: Prior observations from the Chena River (Douglas et al., 2013) | 29 |
| Fig. S19: Prior observations from the Yukon River (Toohey et al., 2016)..... | 30 |
| Fig. S20: Summary of timeseries data from the Yukon River Basin..... | 31 |
| Fig. S21: Timeseries data from the Yukon River at Pilot Station | 32 |
| Fig. S22: Timeseries data from the Yukon River at Stevens Village..... | 33 |
| Fig. S23: Timeseries data from the Yukon River at Eagle | 34 |
| Fig. S24: Timeseries data from the Tanana River at Nenana..... | 35 |
| Fig. S25: Timeseries data from the Porcupine River near Fort Yukon..... | 36 |

References

| | |
|-------------------------|----|
| References | 37 |
|-------------------------|----|

Appendix S1: Ion chromatography

Table S1: Measured major ion concentrations in reference materials and precision of replicate sample measurements. For reference materials, measured values are given as $\mu \pm 1\sigma$ in units of μM , the number of analyses is indicated in parentheses, and measured relative standard deviation (RSD) are given as 1σ . Switzer Falls, an in-house consistency standard, was repeatedly measured but does not have expected values. Reference material variables without listed values, such as Cl^- in CRANBERRY-05 or Mg^{2+} in Switzer Falls, reflect that values were outside the calibration range. Sample values are the mean, median, 1σ standard deviation, and number of analyses for the distribution of RSDs among replicate measurements.

| ANIONS | | | | | | |
|-------------------|--|----------------------|------------|--|---------------------|------------|
| | SO_4^{2-} | | | Cl^- | | |
| <i>References</i> | <i>Expected</i> | <i>Measured</i> | <i>RSD</i> | <i>Expected</i> | <i>Measured</i> | <i>RSD</i> |
| SUPER-05 | 36.2 | 37.1 \pm 1.4 (11) | 3.9% | 39.5 | 42.5 \pm 0.9 (14) | 2.1% |
| CRANBERRY-05 | 92.5 | 96.2 \pm 3.4 (10) | 3.5% | | | |
| MAURI-09 | 39.5 | 38.6 \pm 1.2 (14) | 3.1% | 41.5 | 43.7 \pm 3.2 (17) | 7.3% |
| Switzer Falls | | 318.1 \pm 3.7 (9) | 1.2% | | | |
| <i>Samples</i> | <i>Mean / median of replicate RSDs</i> | | | <i>Mean / median of replicate RSDs</i> | | |
| | 1.9 / 1.1 \pm 2.0% (45) | | | 14.4 / 7.4 \pm 18.4% (64) | | |
| CATIONS | | | | | | |
| | Ca^{2+} | | | Mg^{2+} | | |
| <i>References</i> | <i>Expected</i> | <i>Measured</i> | <i>RSD</i> | <i>Expected</i> | <i>Measured</i> | <i>RSD</i> |
| SUPER-05 | 339.3 | 347.4 (1) | | 116.4 | 120.6 (1) | |
| CRANBERRY-05 | 324.4 | 352.0 \pm 11.7 (2) | 3.3% | 232.0 | 241.8 \pm 0.7 (2) | 0.3% |
| MAURI-09 | 73.4 | 79.6 \pm 9.6 (3) | 12.1% | 30.9 | 31.3 \pm 1.0 (4) | 3.2% |
| Switzer Falls | | | | | | |
| <i>Samples</i> | <i>Mean / median of replicate RSDs</i> | | | <i>Mean / median of replicate RSDs</i> | | |
| | 1.1 / 0.7 \pm 1.1% (15) | | | 1.8 / 1.6 \pm 1.6% (17) | | |
| | Na^+ | | | K^+ | | |
| <i>References</i> | <i>Expected</i> | <i>Measured</i> | <i>RSD</i> | <i>Expected</i> | <i>Measured</i> | <i>RSD</i> |
| SUPER-05 | 62.2 | 63.3 (1) | | 12.9 | 12.5 (1) | |
| CRANBERRY-05 | | | | 17.9 | 18.6 \pm 0.0 (2) | 0.1% |
| MAURI-09 | 95.7 | 97.3 \pm 2.3 (4) | 2.4% | 10.4 | 10.1 \pm 0.4 (6) | 4.4% |
| Switzer Falls | | | | | 89.2 \pm 0.2 (2) | 0.3% |
| <i>Samples</i> | <i>Mean / median of replicate RSDs</i> | | | <i>Mean / median of replicate RSDs</i> | | |
| | 2.2 / 1.8 \pm 2.2% (24) | | | 3.5 / 3.0 \pm 2.6% (13) | | |

Appendix S2: Field context and extended data analysis

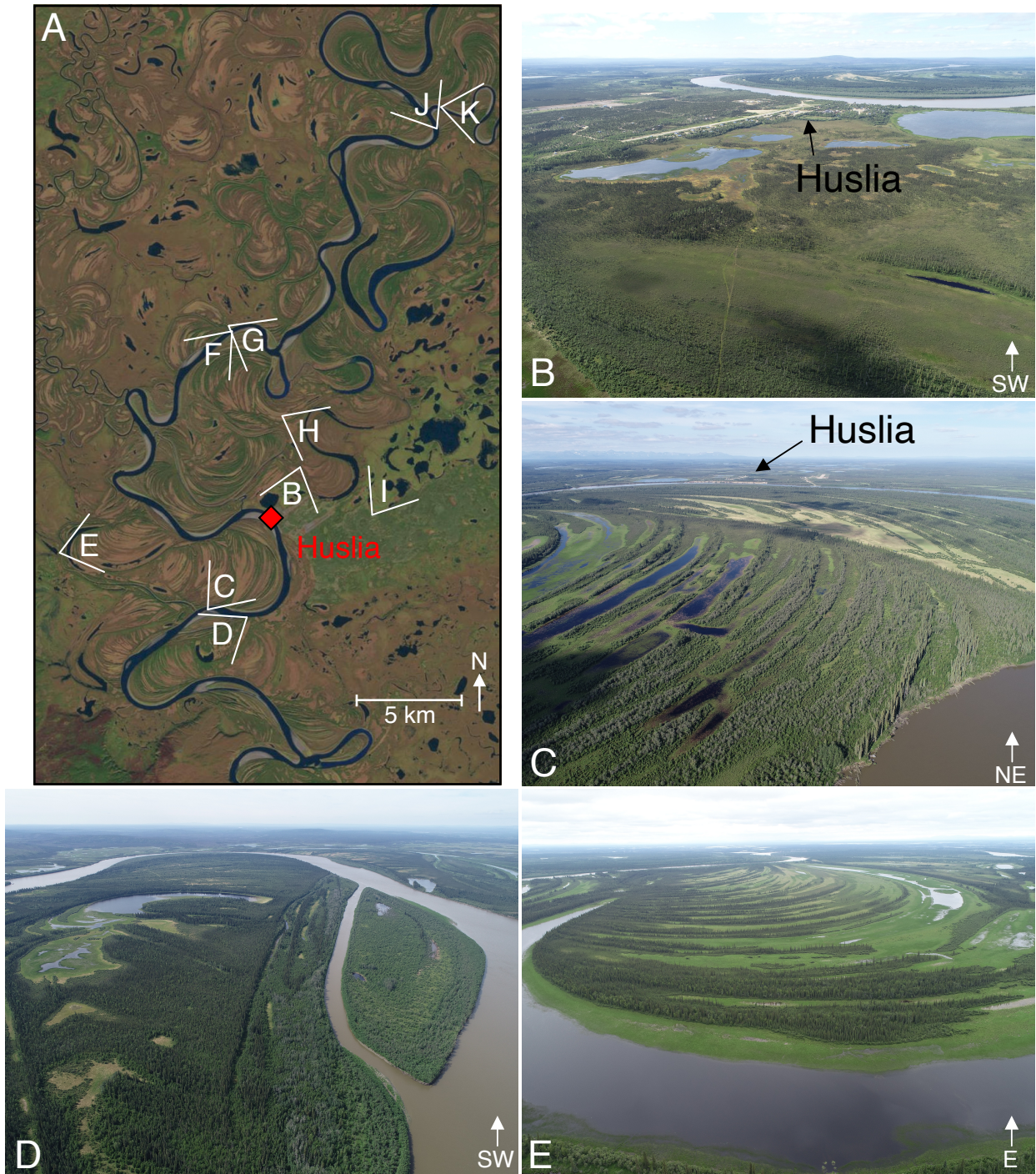


Fig. S1: Overview of field site. (A) Map of field site with approximate locations and image orientations of 10 drone photographs. (B) The village of Huslia. (C) The river bend near Huslia, with scroll bar complex. (D) The most downstream sampled stretch of the Koyukuk River. (E) Looking towards Huslia from the tip of an abandoned meander, with visible scroll bars.